

Article

Numerical Study on Crack Propagation in Brittle Jointed Rock Mass Influenced by Fracture Water Pressure

Yong Li ^{1,*}, Hao Zhou ¹, Weishen Zhu ¹, Shucui Li ¹ and Jian Liu ²

¹ Geotechnical & Structural Engineering Research Center, Shandong University, Jinan 250061, Shandong, China; E-Mails: haozhouchina@gmail.com (H.Z.); zhuw@sdu.edu.cn (W.Z.); lishucui@sdu.edu.cn (S.L.)

² School of Civil Engineering, Shandong University, Jinan 250061, Shandong, China; E-Mail: lj75@sdu.edu.cn

* Author to whom correspondence should be addressed; E-Mail: yongli@sdu.edu.cn; Tel.: +86-531-8839-9320; Fax: +86-531-8839-5428.

Academic Editor: Changle Chen

Received: 8 April 2015 / Accepted: 3 June 2015 / Published: 9 June 2015

Abstract: The initiation, propagation, coalescence and failure mode of brittle jointed rock mass influenced by fissure water pressure have always been studied as a hot issue in the society of rock mechanics and engineering. In order to analyze the damage evolution process of jointed rock mass under fracture water pressure, a novel numerical model on the basis of secondary development in fast Lagrangian analysis of continua (FLAC3D) is proposed to simulate the fracture development of jointed rock mass under fracture water pressure. To validate the feasibility of this numerical model, the failure process of a numerical specimen under uniaxial compression containing pre-existing fissures is simulated and compared with the results obtained from the lab experiments, and they are found to be in good agreement. Meanwhile, the propagation of cracks, variations of stress and strain, peak strength and crack initiation principles are further analyzed. It is concluded that the fissure water has a significant reducing effect on the strength and stability of the jointed rock mass.

Keywords: fracture propagation; jointed rock mass; fracture water pressure; numerical simulation

1. Introduction

To a great extent, it is the nearly ubiquitous presence of fractures that makes the mechanical behavior of rock masses different from that of most engineering materials. These fractures have a controlling influence on the mechanical behavior of rock masses, since existing fractures provide planes of weakness on which further deformation can more readily occur. Fractures also often provide the major conduits through which fluids can flow [1]. As the Chinese economy gradually grows, the Chinese government will begin to construct numerous huge engineering projects, like hydropower stations, mining, tunnels, large-scale underground caverns for energy storage, *etc.* Therefore, the related problems in jointed rock mass will be encountered in the future [2]. A series of cracking processes finally control the overall behavior of the rock, which have prompted extensive experimental studies of pre-cracked specimens of different materials, including rock-like brittle/semi-brittle materials and natural rocks: glass [3], molded gypsum [4], sand-stone-like material [5], granite [6], marble [7], *etc.* Numerous numerical methods have also been used to simulate the fracture development. These methods could be divided into two types: continuous and discontinuous numerical methods. Tang *et al.* [8] developed some numerical methods to simulate the initiation and coalescence of flaws in rock-like materials, including the finite element method (FEM), boundary element method (BEM) and displacement discontinuity method (DDM), and Tang [9] also proposed a new numerical code named RFPA2D (Rock Failure Process Analysis) to simulate the propagation and coalescence of cracks in a rock bridge area. In addition, the discrete element method (DEM) is also used to simulate the mechanical behavior of rock-like materials [10–13]. The above research was not entirely conducted under the conditions of fissure water pressure. Fang and Harrison [14,15] adopted a degradation model to simulate the brittle failure in heterogeneous rocks. Xie *et al.* [16] proposed a micromechanical analysis of damage and related inelastic deformation in saturated porous quasi-brittle materials in 2012. Then, Zhu *et al.* [17] gave a deep discussion about two dissipative processes in microcracks. Bikong *et al.* [18] proposed a micro-macro model for the time-dependent behavior of clayey rocks in 2015. Richardson *et al.* [19] presented a method for simulating quasi-static crack propagation in 2D, which combines XFEM with a simple integration technique and a very general algorithm for cutting triangulated domains. In this paper, to simulate the fissure development of jointed rock mass under fissure water pressure, we propose a novel numerical model on the basis of secondary development in Lagrangian analysis of continua (FLAC3D) [20], which is an explicit finite difference method (FDM). Finally, the numerical model is used to study the fissure development of rock specimens.

2. An Elastic-Brittle Constitutive Model and Hydro-Mechanical Coupling

2.1. An Elastic-Brittle Constitutive Model

As is known to us all, the nonlinear stress-strain relationship of brittle materials, like rock, concrete *etc.*, does not result from plastic deformations. It is caused by the initiation, propagation and coalescence of the micro-cracks in heterogeneous materials. Therefore, it is appropriate to adopt an elastic-damage model to describe the micro-mechanical properties of brittle materials. The behavior of the rock element undergoing failure, as used in the analysis of the behavior of a rock specimens [21,22], may be simplified to either elastic-brittle, elastic-strain softening (a combination of brittle and ductile) or elastic-ductile (plastic) mechanisms, as shown in Figure 1.

The above elastic-plastic model and strain-softening model could not effectively simulate the failure development of rock materials; even some microscopic problems are difficult to be solved due to the large plastic zone appearing in the crack tips. According to the curves of elastic-brittle stress-strain relations, a piecewise function could be used to express the whole process of the stress-strain relations.

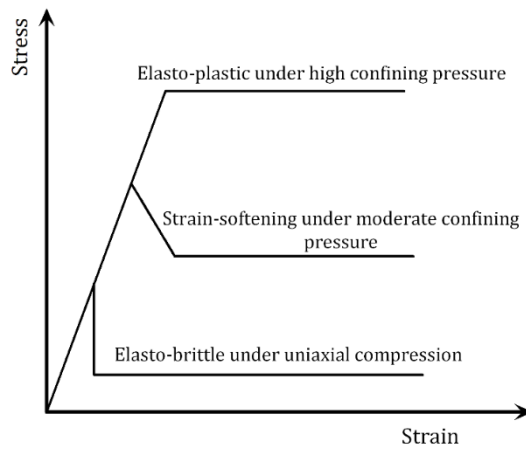


Figure 1. Simplified stress-strain relations of rock elements under different confining pressures within a stressed rock body.

As for the post-failure elements, the mechanical properties must be degraded, and the stress field must be redistributed. Consequently, tensile failure occurs, and cracks are initiated. This model could be effectively used to simulate the complex fissure development in heterogeneous materials. In this elastic-brittle damage model, the specimens under uniaxial tensile loads still have residual strength after they undergo yield strength. This model could be expressed as the following equations:

$$D = \begin{cases} 0, & \varepsilon < \varepsilon_{t0} \\ 1 - \frac{\sigma_i}{\varepsilon \cdot E_0}, & \varepsilon_{t0} \leq \varepsilon \leq \varepsilon_{tu} \\ 1, & \varepsilon > \varepsilon_{tu} \end{cases} \quad (1)$$

$$\sigma_i = \eta \cdot \sigma_t \quad (2)$$

where σ_i is the residual strength; ε_{t0} is the initial damage threshold; ε_{tu} is the limit of tensile strain; η is the residual strength coefficient; D represents the damage variable; and σ_t is the uniaxial tensile strength.

According to Mazars' method [23], the tensile strain ε in Equation (1) could be substituted by an equivalent strain $\bar{\varepsilon}$ in three-dimensional conditions:

$$D = \begin{cases} 0, & \bar{\varepsilon} < \varepsilon_{t0} \\ 1 - \frac{\sigma_i}{\bar{\varepsilon} \cdot E_0}, & \varepsilon_{t0} \leq \bar{\varepsilon} \leq \varepsilon_{tu} \\ 1, & \bar{\varepsilon} > \varepsilon_{tu} \end{cases} \quad (3)$$

where $\bar{\varepsilon} = \sqrt{(\varepsilon_1)^2 + (\varepsilon_2)^2 + (\varepsilon_3)^2}$.

Based on elastic damage mechanics, the stress-strain relations of the constitutive model could be described as the following equations:

$$\sigma_{ij} = \begin{cases} 2G \cdot \varepsilon_{ij} + \lambda \cdot \delta_{ij} \cdot \varepsilon_{kk}, \bar{\varepsilon} < \varepsilon_{t0} \\ \frac{\sigma_i}{\bar{\varepsilon} \cdot E_0} (2G \cdot \varepsilon_{ij} + \lambda \cdot \delta_{ij} \cdot \varepsilon_{kk}), \varepsilon_{t0} \leq \bar{\varepsilon} \leq \varepsilon_{tu} \\ 0, \bar{\varepsilon} > \varepsilon_{tu} \end{cases} \quad (4)$$

where $G = \frac{E_0}{2(1+\nu)}$; $\lambda = \frac{E_0 \cdot \nu}{(1+\nu) \cdot (1-\nu)}$; and $\delta_{ij} = \begin{cases} 1, i = j \\ 0, i \neq j \end{cases}$.

The damage evolution equations of shear failure are expressed as below:

$$D = \begin{cases} 0, \varepsilon_1 < \varepsilon_{c0} \\ 1 - \frac{\sigma_{rc}}{\varepsilon_1 \cdot E_0}, \varepsilon_1 \geq \varepsilon_{c0} \end{cases} \quad (5)$$

where σ_{rc} is the residual strength of shear damage; and ε_{c0} is the strain threshold of shear damage.

Finally, when an element is experiencing shear failure, the equations of the constitutive model could be expressed as below:

$$\sigma_{ij} = \begin{cases} 2G \cdot \varepsilon_{ij} + \lambda \cdot \delta_{ij} \cdot \varepsilon_{kk}, \varepsilon_1 < \varepsilon_{c0} \\ \frac{\sigma_{rc}}{\varepsilon_1 \cdot E_0} (2G \cdot \varepsilon_{ij} + \lambda \cdot \delta_{ij} \cdot \varepsilon_{kk}), \varepsilon_{c0} \leq \varepsilon_1 \leq \varepsilon_{ut} \\ 0, \bar{\varepsilon} > \varepsilon_{ut} \end{cases} \quad (6)$$

2.2. Hydro-Mechanical Coupling of Jointed Rock Mass

The hydro-mechanical coupling of jointed rock mass is realized by the stress equilibrium equation and the continuous seepage equation. The stress equilibrium equation is usually expressed by the principle of virtual work. This means that the virtual work difference of body forces and plane forces at any time is zero:

$$\int \delta \varepsilon^T d\sigma dV - \int \delta u^T df dV - \int \delta u^T dt dS = 0 \quad (7)$$

where $\delta \varepsilon$ is the virtual strain; δu is the virtual displacement; t is the plane force; and f is the body force.

When porous media is considered, the expression of the Biot effective stress is:

$$\sigma' = \sigma - \alpha \bar{p} \quad (8)$$

where σ' is the effective stress; σ is the total stress; α is Biot's coefficient; and \bar{p} is the average stress of the fluid. Biot's coefficient would evolve with the damage process, but it is very difficult to obtain its variation principle during the coupling process. According to the research results of Walsh [24] and Zhao [25], Biot's coefficient is between zero and one.

The constitutive model could be expressed by the strain increment:

$$d\sigma' = D_{ep}(d\varepsilon - d\varepsilon_l) \quad (9)$$

where D_{ep} represents an elastic-plastic matrix; and $d\varepsilon_l$ is the particle compression induced by pore flow. Here, this is calculated as the following equation:

$$\varepsilon = \sigma'(1 - D)E_0 \quad (10)$$

The continuous seepage equation is expressed as below based on a hypothesis of the Darcy flow:

$$S_w \left[m^T - \frac{m^T D_{ep}}{3K_s} \right] \frac{d\varepsilon}{dt} - \nabla^T \left[k_0 k_r \left(\frac{\nabla p_w}{p_w} - g \right) \right] + \left\{ \zeta n + n \frac{S_w}{k_w} + S_w \left[\frac{1-n}{3K_s} - \frac{m^T D_{ep} m}{(3K_s)^2} \right] (S_w + p_w \zeta) \right\} \frac{dp_w}{dt} = 0 \quad (11)$$

where S_w is the degree of saturation; p_w is the pore water pressure; $\zeta = \frac{ds_w}{dp_w}$; k_0 is the initial permeability coefficient tensor; k_r is the permeability coefficient; g is the gravity acceleration vector; n is the porosity; and k_w is the bulk modulus of water. The above equations provide the theoretical fundamentals in hydro-mechanical coupling of jointed rock mass.

3. Implementation of the Elastic-Brittle Coupling Model in FLAC3D

A survey of commercially available codes shows that the program fast Lagrangian analysis of continua (FLAC3D), produced by Itasca Consulting Group [20], uses an explicit finite difference scheme for the analysis of problems in engineering mechanics. FLAC3D implements an explicit time marching scheme to solve Newton's second law to describe material deformation and embodies a number of basic constitutive models for use in the analysis of the mechanical behavior of geo-materials. Based on these, users can incorporate their own constitutive models by writing a function using a built-in programming language, which is called the FISH language. This provides an easy way to enhance the program, and hence, solve complex problems in rock mechanics and rock engineering. Thus, FLAC has been adopted for the implementation of the elastic-brittle coupling model. Figure 2 shows the procedure for the implementation of the elastic-brittle coupling model in FLAC3D.

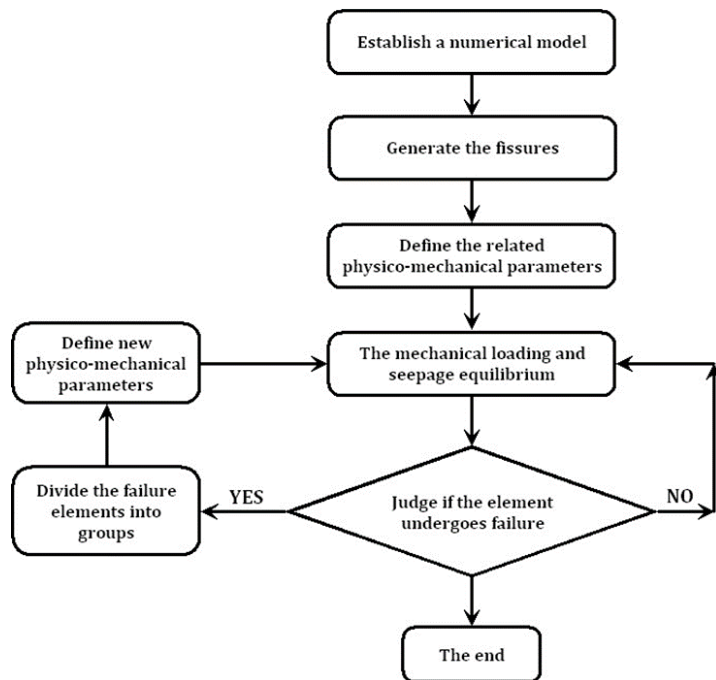


Figure 2. The procedure for the implementation of the elastic-brittle coupling model in Lagrangian analysis of continua (FLAC3D).

4. Numerical Simulations on the Specimens Containing Precast Fissures

4.1. A Two-Dimensional Numerical Simulation

The dimensions of the length, height and thickness in the two-dimensional numerical model shown in Figure 3 are 50 mm, 100 mm and 1 mm, respectively. This numerical model is divided into 7524 elements. It contains two types of media, the intact rock mass and precast fissures. The two parallel fissures are located in the center of the model. The vertical distance between them is 16 mm; the length of the fissure is 18 mm; the thickness is 1 mm; and the dip angle is 45°. The whole numerical model is freely meshed by hexahedral elements. The related physico-mechanical parameters are shown in Table 1.

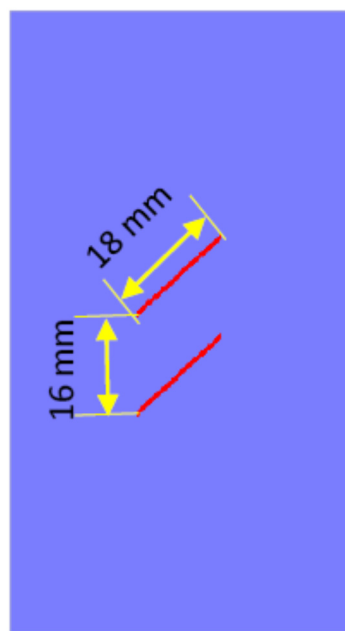


Figure 3. The two-dimensional numerical model.

Table 1. Physico-mechanical parameters of intact rock mass and precast fissure.

Rock types	Elastic modulus (GPa)	Poisson's ratio	Tensile strength (MPa)	Cohesion (MPa)	Friction angle (°)	Dilatancy angle (°)
Intact rock mass	45.0	0.25	0.9	1.6	40	0
Precast fissure	1.5	0.35	0.5	0.8	20	0

Next, the elasto-plastic model, the strain-softening model and the elastic-brittle model are also used to simulate the fracture development under uniaxial compression. Figure 4 shows the numerical simulation results. Figure 4a is obtained by the elasto-plastic model. Although the failure occurs near the fissure tips and large-area plastic zones appear, the development of the secondary cracks could not be better observed. Figure 4b is obtained by the strain softening model. Although the plastic zone becomes smaller, it has the same difficulty as Figure 4a. Figure 4c is obtained by the elastic-brittle model. We find that the simulation results are absolutely different with those obtained by the above two models. We observe the development of secondary cracks, and no large-area plastic zones appear, which is extremely close to the results obtained in the laboratory testing specimens [26].

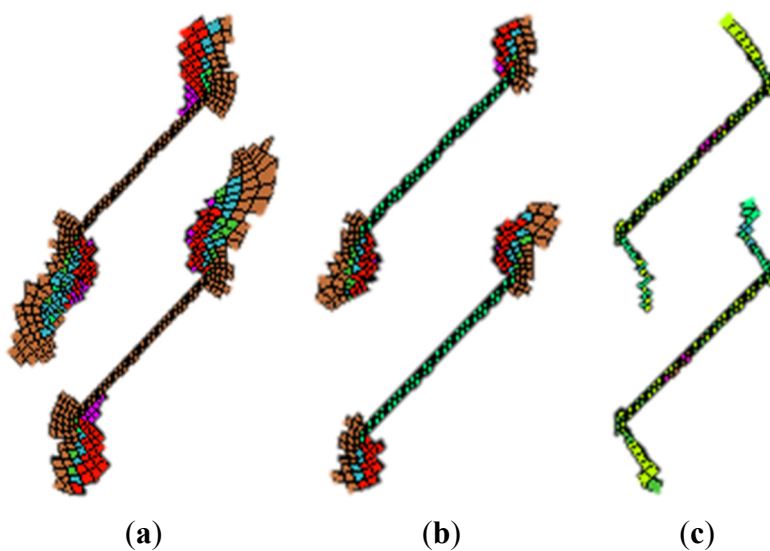


Figure 4. Numerical simulation results using elasto-plastic, strain softening and elastic brittle models. (a) Plastic zones obtained by elasto-plastic model; (b) Plastic zones obtained by strain-softening model; (c) Plastic zones obtained by elastic-brittle model.

From the numerical results, it is concluded that the elastic-brittle model is more appropriate to simulate the fracture development of brittle geo-materials.

4.2. Three-Dimensional Numerical Simulations

The three-dimensional numerical model adopts a cuboid model, as shown in Figure 5, and the dimensions of the length, width and height are 50 mm, 50 mm and 100 mm, respectively. Two elliptic mica sheets are used to simulate the double fissures, which is more appropriate than the metal sheets in mechanical behavior. The long axis, short axis and thickness of the elliptic fissure are 18 mm, 15 mm and 1 mm. The fissure planes have an inclination angle of 45° to the horizontal plane, and the vertical distance between them is 16 mm. The rolling constraint is fixed to the top and bottom surfaces. In order to clearly observe the fissure development, super fine meshes are generated, and the number of elements is 270,603, as shown in Figure 6. The uniaxial loading is applied on the top and bottom surfaces. The related physico-mechanical parameters are also shown in Table 1.

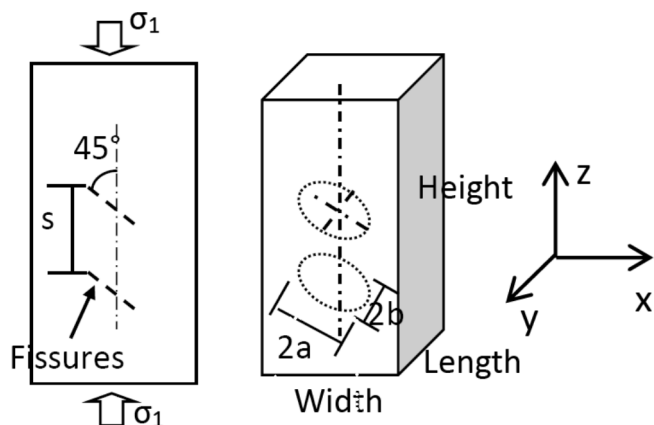


Figure 5. Location of double parallel fissures.

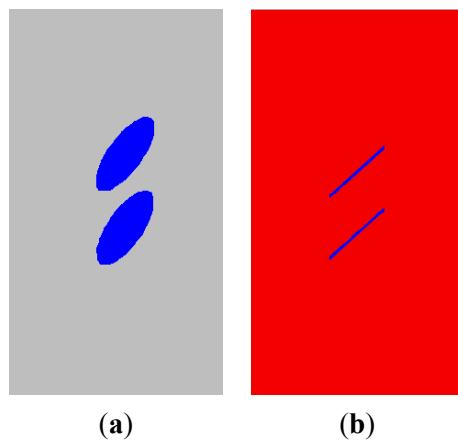


Figure 6. The three-dimensional model. **(a)** A side view; **(b)** A front view.

When the elastic brittle numerical model is used to perform the numerical simulations on the fissure development in the specimens, the following essentials should be noticed. As for the elements experiencing shear failures, their residual shear strength should be reduced to five percent of the original shear strength, and for the elements experiencing tensile failures, their tensile strength and cohesion should be reduced to only one percent of the original values. However, whatever failures the elements experience, the friction angle should be kept invariant, and the bulk and shear modulus should be degraded to the same order of magnitude.

4.2.1. Case Study I: Numerical Analysis on the Double-Fissured Specimen under Uniaxial Compression without Fissure Water Pressure

In this case, the double-fissured specimen under uniaxial compression without fissure water pressure is numerically simulated based on the elastic brittle model. Figure 7 shows the fissure development and the profile of the secondary cracks.

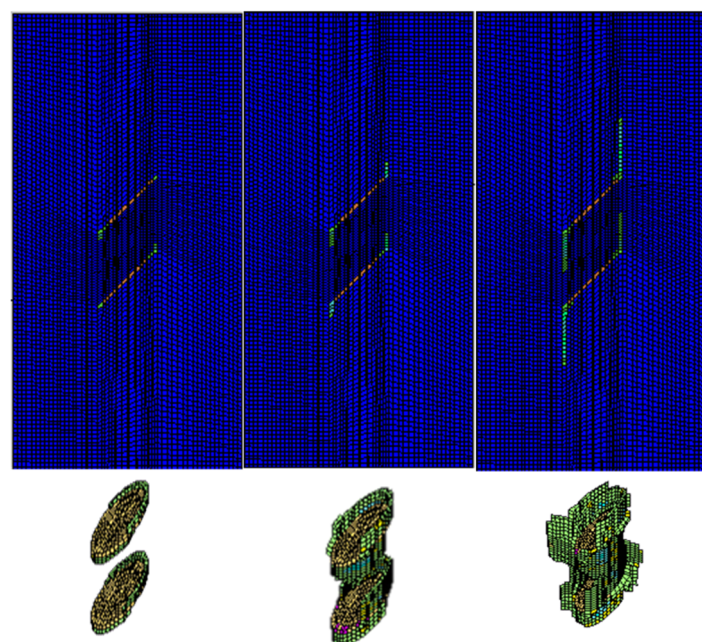


Figure 7. The fissure development and profiles of secondary cracks.

During the beginning of uniaxial compressive loading, we could observe that small encapsulated failure planes initiate near the long-axis tips of the elliptical fissure sheet; the secondary cracks start to extend along the loading direction, and the wing cracks are formed. Although the secondary cracks initiate and extend gradually, they have no coalescence areas, and the rock mass between the two fissure sheets remains intact at this stage. As the loading continues to increase to 44.7% of the peak compressive strength, a major failure zone induced by the propagation of secondary cracks is formed in the rock bridge. Afterwards, the failure planes start to extend along the fissure edges until the final failure occurs. The peak compressive strength is 58.2 MPa.

The complete stress-strain curve is drawn in Figure 8. In the beginning of loading, the specimen is in the linear elastic stage. When the curves approach the peak values, the axial and transversal strains increase faster, and the specimen appears dilatancy. When the peak strength appears, the stress decreases rapidly. The whole process behaves with the typical characteristics of brittle materials.

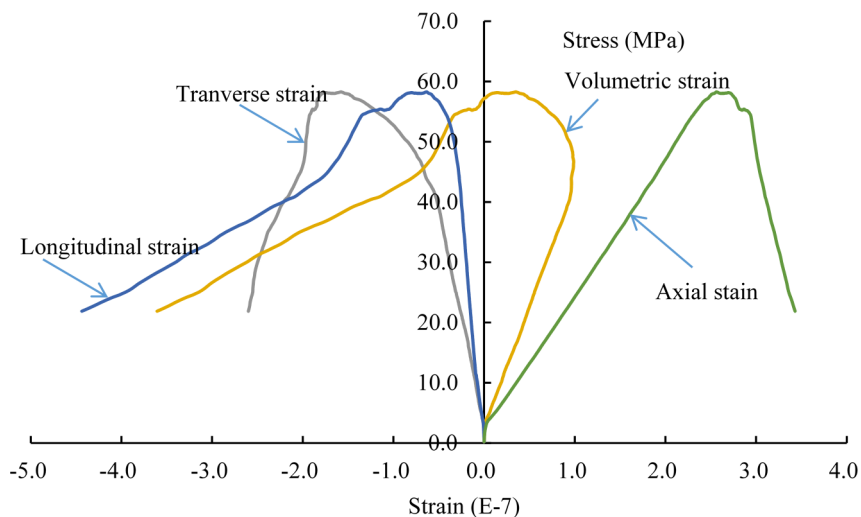


Figure 8. The complete stress-strain curve of the double-fissured specimen under uniaxial compression without fissure water pressure.

4.2.2. Case Study II: Numerical Analysis on the Double-Fissured Specimen under Uniaxial Compression Considering Fissure Water Pressure

In this case, the double-fissured specimen under uniaxial compression considering fissure water pressures is numerically simulated based on the elastic brittle coupling model. According to the actual laboratory experiments, two representative fissure water pressures are considered. One is 3.5 percent of the uniaxial peak strength ($3.5\% \sigma_a$), and the other is $3.5\% \sigma_a$. Figure 9 shows the fissure development and profiles of secondary cracks under fissure water pressure ($3.5\% \sigma_a$). Figure 10 is the complete stress-strain curve under fissure water pressure ($3.5\% \sigma_a$). Figures 11 and 12 show the numerical results under fissure water pressure ($7\% \sigma_a$).

The following results could be concluded from the numerical simulations:

(1) When the fissure water pressure is equal to $3.5\% \sigma_a$, the final uniaxial peak strength is 59.0 MPa. At the beginning of loading, we could find that the fissure development has a similar principle. As the loading continues to increase to 41.3% of the peak compressive strength, a major failure zone induced

by the propagation of secondary cracks is formed in the rock bridge. Therefore, it is concluded that the fissure water pressure ($3.5\% \sigma_a$) has a slight impact on the fissure development.

(2) As the fissure water pressure is increased to $7\% \sigma_a$, its impact could not be neglected. The final uniaxial peak strength has obviously been decreased to 42.2 MPa. The cracks initiate and extend while the uniaxial load is 2.11 MPa. As the loading continues to increase, the cracks extend rapidly, because the fissure water pressure intensifies the tensile effects at the fissure tips. When the uniaxial loading is 27.85 MPa, a major failure zone induced by the propagation of secondary cracks is formed in the rock bridge. Afterwards, the failure planes start to extend along the fissure edges until the final failure occurs.

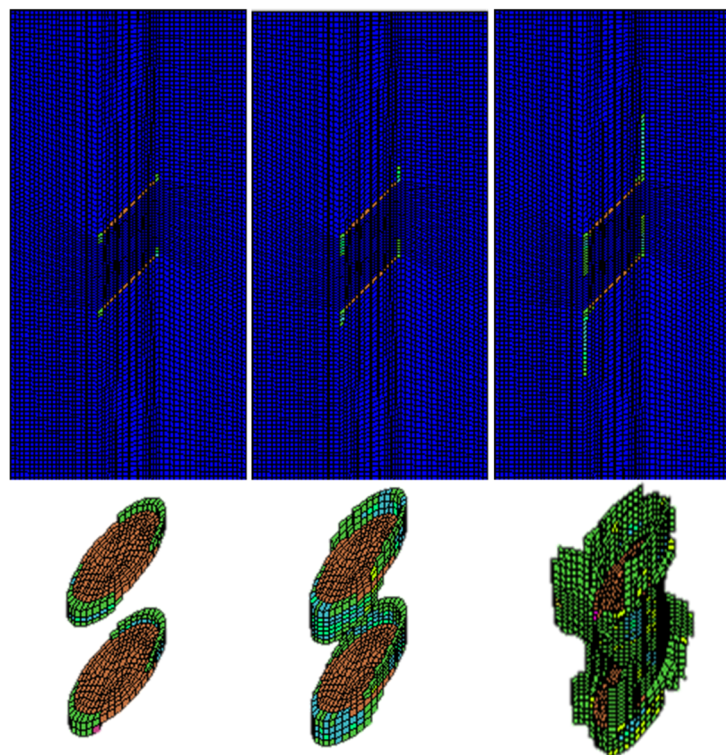


Figure 9. Fissure development and profiles of secondary cracks under fissure water pressure ($3.5\% \sigma_a$).

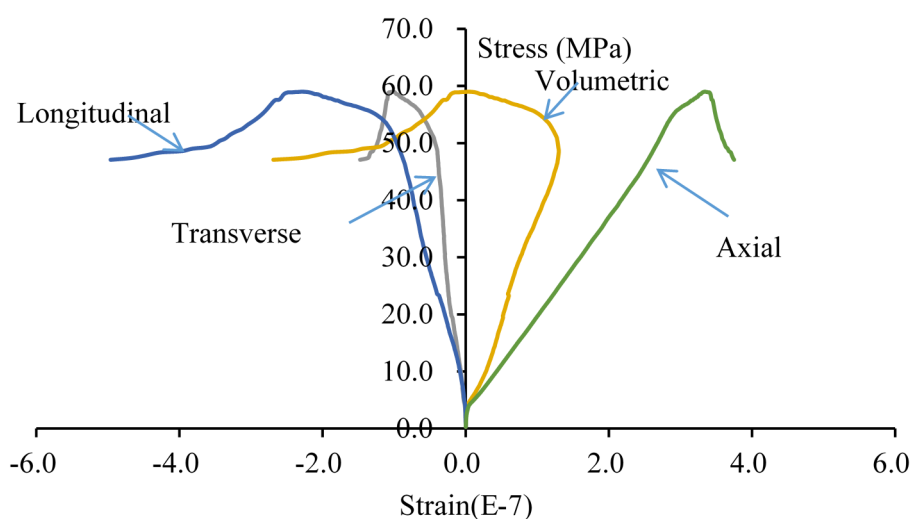


Figure 10. The complete stress-strain curve of the double-fissured specimen under uniaxial compression under fissure water pressure ($3.5\% \sigma_a$).

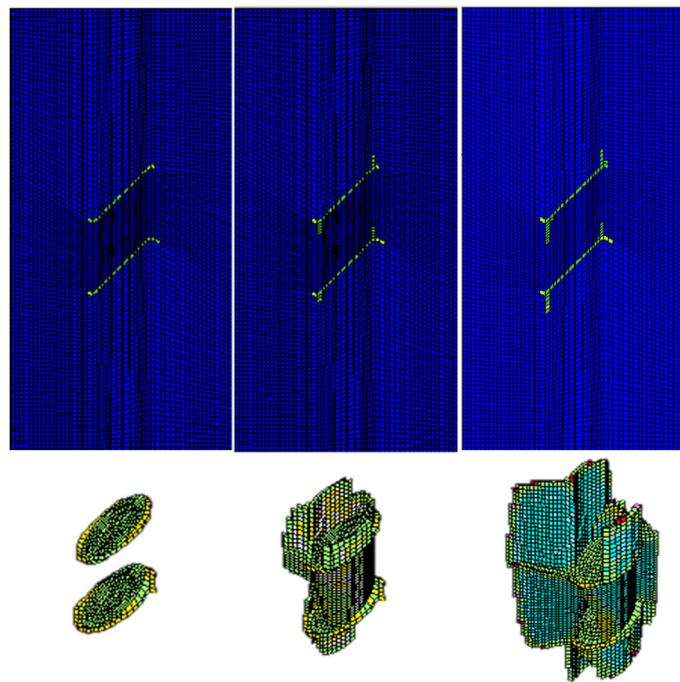


Figure 11. Fissure development and profiles of secondary cracks under fissure water pressure (7% σ_0).

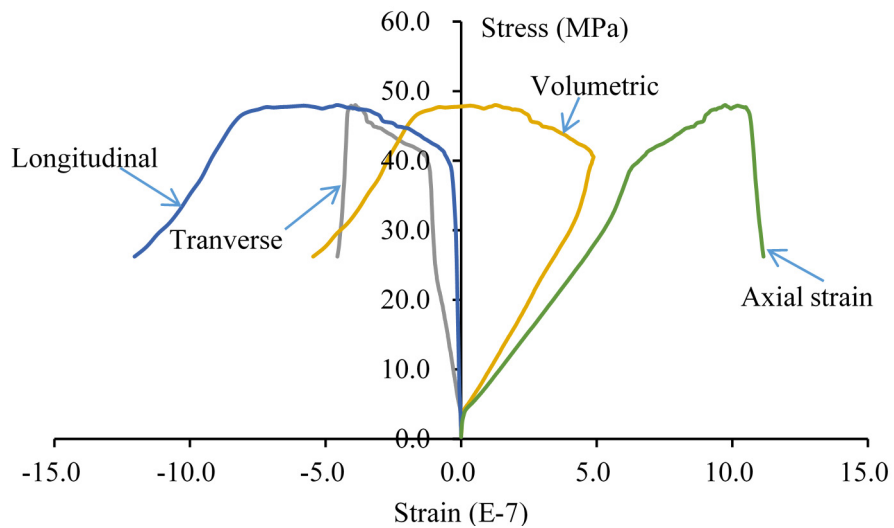


Figure 12. The complete stress-strain curve of the double-fissured specimen under uniaxial compression under fissure water pressure (7% σ_0).

5. Conclusions

(1) An elastic brittle coupling constitutive model on the basis of secondary development in FLAC3D is proposed to simulate the fracture development of jointed rock mass under fracture water pressure. The two-dimensional numerical results are found to be in good agreement with the laboratory results.

(2) The fissure water pressure has a significant impact on the peak strength of pre-cracked rock specimen. When the value is small, the peak strength may be increased a little. However, when it increases to a bigger value, the peak strength would be decreased rapidly, and a large-area failure zone would appear in the rock bridge. The failure planes start to extend along the fissure edges until the final failure occurs.

Acknowledgments

The work was supported by the National Science and Technology Support Program of China (2015BAB07B05), the Natural Science Foundation of Shandong Province (BS2012NJ006) and the Specialized Research Fund for the Doctoral Program for Higher Education (No. 20110131120034). We would also like to express our sincere gratitude to the editor and the two anonymous reviewers for their valuable contributions to this paper.

Author Contributions

This present research article is based on the research work of Yong Li and Hao Zhou. During the research work, Weishen Zhu, Shucui Li and Jian Liu have provided substantial contributions to the theoretical innovation and experimental guidance. Hao Zhou performed a lot of work in laboratory experiments and Yong Li conducted the numerical simulation and analyzed the related data. Finally, Yong Li finished the whole writing of this paper.

Conflicts of Interest

The authors of the paper declare that there is no conflict of interest regarding the publication of this paper. The authors do not have a direct financial relation with the commercial identity that might lead to a conflict of interest for any of the authors.

References

1. Jaeger, J.C.; Cook, N.G.W. *Fundamentals of Rock Mechanics*, 3rd ed.; Chapman and Hall: London, UK, 1979.
2. Li, Y.; Zhu, W.S.; Fu, J.W.; Guo, Y.H.; Qi, Y.P. A damage rheology model applied to analysis of splitting failure in underground caverns of Jinping I hydropower station. *Int. J. Rock Mech. Min. Sci.* **2014**, *71*, 224–234.
3. Hoek, E.; Bieniawski, Z.T. Brittle fracture propagation in rock under compression. *Int. J. Fract.* **1965**, *1*, 137–155.
4. Bobet, A. The initiation of secondary cracks in compression. *Eng. Fract. Mech.* **2000**, *66*, 187–219.
5. Mughieda, O.; Alzo’ubi, A.K. Fracture mechanisms of offset rock joints—A laboratory investigation. *Geotech. Geolog. Eng.* **2004**, *22*, 545–562.
6. Miller, J.T.; Einstein, H.H. Crack coalescence tests on granite. In Proceedings of 42nd US Rock Mechanics Symposium, San Francisco, CA, USA, 28 June–2 July 2008; ARMA-08-162.
7. Li, Y.P.; Chen, L.Z.; Wang, Y.H. Experimental research on pre-cracked marble under compression. *Int. J. Solids Struct.* **2005**, *42*, 2505–2516.
8. Tang, C.A.; Lin, P.; Wong, R.H.C.; Chau, K.T. Analysis of crack coalescence in rock-like materials containing three flaws-part II: Numerical approach. *In. J. Rock Mech. Min. Sci.* **2001**, *38*, 925–939.
9. Tang, C.A.; Kou, S.Q. Crack propagation and coalescence in brittle materials under compression. *Eng. Fract. Mech.* **1998**, *61*, 311–324.
10. Lee, H.; Jeon, S. An experimental and numerical study of fracture coalescence in pre-cracked specimens under uniaxial compression. *Int. J. Solids Struct.* **2011**, *48*, 979–999.

11. Yang, S.Q.; Huang, Y.H.; Jing, H.W.; Liu, X.R. Discrete element modeling on fracture coalescence behavior of red sandstone containing two unparallel fissures under uniaxial compression. *Eng. Geol.* **2014**, *178*, 28–48.
12. Manouchehrian, A.; Sharifzadeh, M.; Marji, M.F.; Gholamnejad, J. A bonded particle model for analysis of the flaw orientation effect on crack propagation mechanism in brittle materials under compression. *Arch. Civ. Mech. Eng.* **2014**, *14*, 40–52.
13. Mughieda, O.; Omar, M.T. Stress analysis for rock mass failure with offset joints. *Geotech. Geol. Eng.* **2008**, *26*, 543–552.
14. Fang, Z.; Harrison, J.P. Development of a local degradation approach to the modeling of brittle fracture in heterogeneous rocks. *Int. J. Rock Mech. Min. Sci.* **2002**, *39*, 443–457.
15. Fang, Z.; Harrison, J.P. Application of a local degradation model to the analysis of brittle fracture of laboratory scale rock specimens under triaxial conditions. *Int. J. Rock Mech. Min. Sci.* **2002**, *39*, 459–476.
16. Xie, N.; Zhu, Q.Z.; Shao, J.F.; Xu, L.H. Micromechanical analysis of damage in saturated quasi brittle materials. *Int. J. Solids Struct.* **2012**, *49*, 919–928.
17. Zhu, Q.Z.; Shao, J.F. A refined micromechanical damage–friction model with strength prediction for rock-like materials under compression. *Int. J. Solids Struct.* **2015**, *60–61*, 75–83.
18. Bikong, C.; Hoxha, D.; Shao, J.F. A micro-macro model for time-dependent behavior of clayey rocks due to anisotropic propagation of microcracks. *Int. J. Plast.* **2015**, *69*, 73–88.
19. Richardson, C.L.; Hegemann, J.; Sifakis, E.; Hellrung, J.; Teran, J.M. An XFEM method for modeling geometrically elaborate crack propagation in brittle materials. *Int. J. Numer. Methods Eng.* **2011**, *88*, 1042–1065.
20. *Fast Lagrangian Analysis of Continua in 3-Dimensions*; version 5.0, manual; Itasca Consulting Group Inc: Itasca, MS, USA, 2012.
21. Fang, Z. A Local Degradation Approach to The Numerical Analysis of Brittle Fracture in Heterogeneous Rocks. Ph.D. Thesis, University of London, London, UK, 6 May 2001.
22. Fang, Z.; Harrison, J.P. A mechanical degradation index for rock. *Int. J. Rock Mech. Min. Sci.* **2001**, *38*, 1193–1199.
23. Mazars, J.; Pijaudier-Cabot, G. Continuum damage theory-application to concrete. *J. Eng. Mech. ASCE* **1989**, *115*, 345–365.
24. Walsh, J.B. Effect of pore pressure and confining pressure on fracture permeability. *Int. J. Rock Mech. Min. Sci. Geom. Abstr.* **1981**, *18*, 429–435.
25. Zhao, Y.S.; Hu, Y.Q.; Zhao, B.H.; Yang, D. Coupled mathematical model for solid deformation and gas seepage of rock matrix-fractured media and its applications. *J. China Coal Soc.* **2003**, *28*, 41–45.
26. Guo, Y.S.; Wong, R.H.C.; Zhu, W.S.; Chau, K.T.; Li, S.C. Study on fracture pattern of open surface-flaw in gabbro. *Chin. J. Rock Mech. Eng.* **2007**, *26*, 525–531.